Inorg. Chem. **2006**, *45*, 7935–7942

Inorganic Chemistry
Article

Influence of the Reaction Conditions on the Self-assembly of Lead(II) 5-Sulfosalicylate Coordination Polymers with Chelating Amine Ligands

Sai-Rong Fan and Long-Guan Zhu*

Department of Chemistry, Zhejiang University, Hangzhou 310027, People's Republic of China

Received May 19, 2006

The synthesis and crystal structures of [Pb(Hssal)(2,2′-bipy)(DMF)]$_n$ (**1**), [Pb(Hssal)(2,2′-bipy)(H_2O)]$_n$ (**2**), [Pb(Hssal)-(phen)(DMF)]$_n$ (**3**), and [Pb_3(ssal)$_2$(phen)$_3$]$_n$ (**4**) were reported, where Hssal^{2-} and ssal^{3-} are doubly and fully deprotonated 5-sulfosalicylates, 2,2′-bipy is 2,2′-bipyridine, and phen is 1,10-phenanthroline. Compounds **1**–**4** were synthesized by the various reaction conditions, such as reaction temperature, molar ratio, and pH, and these structures are formed by infinite chains or layers where Pb^{II} ions are linked by Hssal^{2-} or ssal^{3-} bridges. Compound **1**, which has a ladderlike chain, was formed in DMF/H_2O. Compound **2** with a H_2O molecule coordinated to Pb^{II} was prepared by a hydrothermal reaction. Compounds **3** and **4** were synthesized in a higher pH compared to compounds **1** and **2**, containing the 2,2′-bipy ligand. In **1**–**3**, 5-sulfosalicylates are doubly deprotonated, whereas in **4**, 5-sulfosalicylate is fully deprotonated. Coordination modes of Hssal^{2-} and ssal^{3-} ligands in **1**–**4** are novel and are first reported in this presentation. Although compounds **1** and **3** have the same structural topology, their aromatic–aromatic interactions are significantly different. The coordination spheres of Pb^{II} ions in **1** and **3** are holodirected, whereas in **2** and **4**, they feature somewhat hemidirected properties with small holes or gaps. Compound **4** exhibits some interesting features that (1) there is not any solvent in the structure, (2) there are extensively aromatic–aromatic stacking interactions among aromatic rings, and (3) there is also a weak interaction between Pb^{II} atoms in the trinuclear motif.

Introduction

Recently, increasing attention has been devoted to the coordination chemistry of 5-sulfosalicylic acid (H_3ssal) in both structural and biological interests.[1,2] 5-Sulfosalicylic acid possesses three functional groups, $-SO_3H$, $-COOH$, and $-OH$, and can be partly (H_2ssal$^-$ and Hssal^{2-}) or fully (ssal^{3-}) deprotonated, which can perform a wide range of coordination modes. Charts 1 and 2 demonstrate the coordination modes of the doubly and fully deprotonated 5-sulfosalicylates in recently reported metal complexes, respectively.[3,4] On the other hand, Pb^{II} complexes have been increasingly studied owing to their interests in environmental protection and as a stereochemically active lone pair of electrons;[5−8] the coordination sphere of the Pb^{II} ion can be classified as a hemi- or holodirected configuration,[9] which is important in structural assembly, electron charge transfer, and physical or chemical properties.[9−12] Therefore, the combination of Pb^{II} and 5-sulfosalicylate was used to study the configuration activity of valence-shell electron lone pairs and their diverse structural topologies. To the best of our

---

* To whom correspondence should be addressed. E-mail: chezlg@zju.edu.cn. Fax: +86-571-87951895. Tel: +86-571-87963867.

(1) (a) Toraishi, T.; Aoyagi, N.; Nagasaki, S.; Tanaka, S. *Dalton Trans.* **2004**, 3495. (b) Ma, J. F.; Yang, J.; Li, L.; Zheng, G. L.; Liu, J. F. *Inorg. Chem. Commun.* **2003**, *6*, 581. (c) Marzotto, A.; Clemente, D. A.; Gerola, T.; Valle, G. *Polyhedron* **2001**, *20*, 1079.

(2) (a) Zheng, S. L.; Zhang, J. P.; Chen, X. M.; Ng, S. W. *J. Solid State Chem.* **2003**, *172*, 45. (b) Zheng, S. L.; Tong, M. L.; Zhu, H. L.; Fang, Y.; Chen, X. M. *J. Chem. Soc., Dalton Trans.* **2001**, 2049.

(3) (a) Li, J. F.; Zhao, Y. J.; Li, X. H.; Hu, M. L. *Acta Crystallogr.* **2004**, *E60*, m1210. (b) Hecht, E. *Acta Crystallogr.* **2004**, *E60*, m1286. (c) Chen, Z. F.; Shi, S. M.; Hu, R. X.; Zhang, M.; Liang, H.; Zhou, Z. Y. *Chin. J. Chem.* **2003**, *21*, 1059. (d) Fan, S. R.; Xiao, H. P.; Zhu, L. G. *Acta Crystallogr.* **2006**, *E62*, m18. (e) Fan, S. R.; Zhu, L. G. *Acta Crystallogr.* **2005**, *E61*, m2480. (f) Fan, S. R.; Zhu, L. G.; Xiao, H. P.; Ng, S. W. *Acta Crystallogr.* **2005**, *E61*, m377. (g) Ma, W. X.; Qian, B. H.; Gao, J.; Xu, X. Y.; Lu, L. D.; Yang, X. J.; Wang, X.; Song, H. B. *Chin. J. Inorg. Chem.* **2005**, *21*, 612. (h) Ma, J. F.; Yang, J.; Li, S. L.; Song, S. Y.; Zhang, H. J.; Wang, H. S.; Yang, K. Y. *Cryst. Growth Des.* **2005**, *5*, 807.

(4) (a) Wang, W. G.; Zhang, J.; Song, L. J.; Ju, J. F. *Inorg. Chem. Commun.* **2004**, *7*, 858. (b) Sun, H. Y.; Huang, C. H.; Jin, X. L.; Xu, G. X. *Polyhedron* **1995**, *14*, 1201. (c) Fan, S. R.; Zhu, L. G. *Acta Crystallogr.* **2005**, *E61*, m174. (d) Wang, X. Q.; Zhang, J.; Li, Z. J.; Wen, Y. H.; Cheng, J. K.; Yao, Y. G. *Acta Crystallogr.* **2004**, *C60*, m657. (e) Fan, S. R.; Cai, G. Q.; Zhu, L. G.; Xiao, H. P. *Acta Crystallogr.* **2005**, *C61*, m177. (f) Liu, B.; Wang, Z. J.; Huang, S. P.; Yang, B. S. *Acta Crystallogr.* **2006**, *E62*, m608. (g) Fan, S. R.; Zhu, L. G. *Acta Crystallogr.* **2005**, *E61*, m2080.

10.1021/ic060871v CCC: $33.50

Chart 1. Coordination Modes of Doubly Deprotonated 5-Sulfosalicylates in Recent Reports

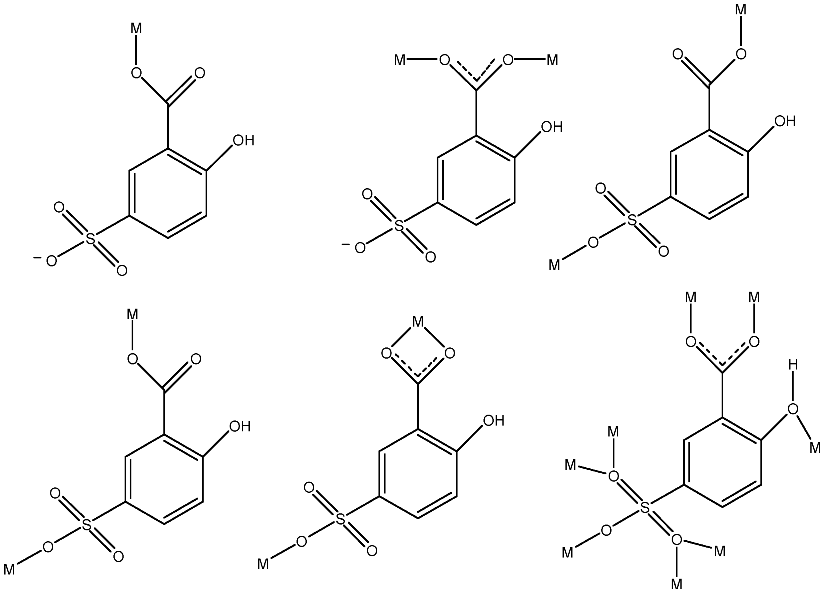

Chart 2. Coordination Modes of Fully Deprotonated 5-Sulfosalicylates in Recent Reports

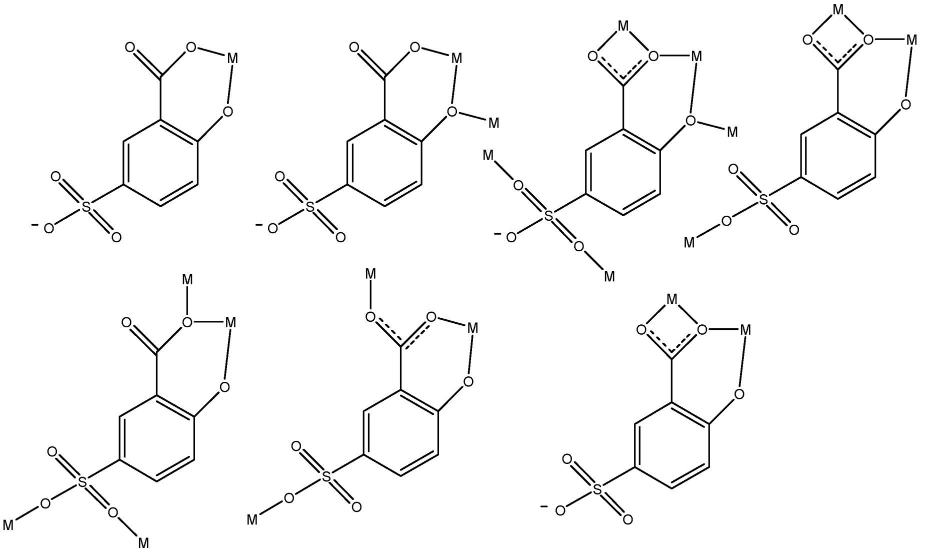

knowledge, only one Pb^{II} complex with the H_3ssal ligand was reported, $[Pb(Hssal)(phen)(H_2O)]_2$ (**5**).[3a] Hence, in the past 3 years, we have paid our attention to the synthesis of lead(II) 5-sulfosalicylate compounds with chelating aromatic amine ligands [2,2′-bipyridine (2,2′-bipy) and 1,10-phenanthroline (phen)] but have compositional and structural diversity. Herein, we present syntheses, structures, properties, and weak interactions of four polymeric Pb^{II} complexes synthesized by various reaction conditions, namely, $[Pb(Hssal)(2,2'\text{-bipy})(DMF)]_n$ (**1**), $[Pb(Hssal)(2,2'\text{-bipy})(H_2O)]_n$ (**2**), $[Pb(Hssal)(phen)(DMF)]_n$ (**3**), and $[Pb_3(ssal)_2(phen)_3]_n$ (**4**).

Experimental Section

Materials and Instruments. All chemicals were purchased from Acros Organics and were used as received without purification. Microanalyses (C, H, and N) were carried out on a Perkin-Elmer analyzer model 1110. IR spectra were recorded as KBr pellets in the 400−4000-cm^{-1} region using a Nicolet Nexus 470 spectro-

---

(5) (a) Shimoni-Livny, L.; Glusker, J. P.; Bock, C. W. *Inorg. Chem.* **1998**, *37*, 1853. (b) Parr, J. *Polyhedron* **1997**, *16*, 551.

(6) (a) Payne, J. C.; Horst, M. A.; Godwin, H. A. *J. Am. Chem. Soc.* **1999**, *121*, 6850. (b) Magyar, J. S.; Weng, T. C.; Stern, C. M.; Dye, D. F.; Rous, B. W.; Payne, J. C.; Bridgewater, B. M.; Mijovilovich, A.; Parkin, G.; Zaleski, J. M.; Penner-Hahn, J. E.; Godwin, H. A. *J. Am. Chem. Soc.* **2005**, *127*, 9495. (c) Ambrosi, G.; Formica, M.; Fusi, V.; Giorgi, L.; Guerri, A.; Micheloni, M.; Paoli, P.; Pontellini, R.; Rossi, P. *Inorg. Chim. Acta* **2003**, *356*, 203. (d) Kurtaran, R.; Yildirim, L. T.; Azaz, A. D.; Namli, H.; Atakol, O. *J. Inorg. Biochem.* **2005**, *99*, 1937.

(7) (a) Morsali, A.; Mahjoub, A. R. *Solid State Sci.* **2005**, *7*, 1429. (b) Morsali, A.; Mahjoub, A. R. *Inorg. Chem. Commun.* **2004**, *7*, 915. (c) Morsali, A.; Mahjoub, A. R. *Polyhedron* **2004**, *23*, 2427.

(8) Kavallieratos, K.; Rosenberg, J. M.; Bryan, J. C. *Inorg. Chem.* **2005**, *44*, 2573.

(9) Hancock, R. D.; Reibenspies, J. H.; Maumela, H. *Inorg. Chem.* **2004**, *43*, 2981.

(10) Nordell, K. J.; Schultz, K. N.; Higgins, K. A.; Smith, M. D. *Polyhedron* **2004**, *23*, 2161.

(11) Panda, S.; Singh, H. B.; Butcher, R. J. *Inorg. Chem.* **2004**, *43*, 8532.

(12) Esteban-Gomez, D.; Ferreiros, R.; Fernandez-Martinez, S.; Avecilla, F.; Platas-lglesias, C.; de Blas, A.; Rodriguez-Blas, T. *Inorg. Chem.* **2005**, *44*, 5428.

photometer. Thermogravimetric analyses (TGA) were studied by a Delta Series TA-SDT Q600 in a N_2 atmosphere in the temperature range between room temperature and 500 °C (heating rate = 10 °C·min^{-1}) using Al crucibles. The photoluminescence study was carried out on a powdered sample in the solid state at room temperature using a Hitachi 850 spectrometer.

Synthesis of [Pb(Hssal)(2,2′-bipy)(DMF)]$_n$ (1). A mixture of $Pb(CH_3COO)_2 \cdot 3H_2O$ (0.097 g, 0.26 mmol), 5-sulfosalicylic acid dihydrate (0.130 g, 0.51 mmol), and 2,2′-bipy (0.031 g, 0.20 mmol) in a solution of water (10 mL) and dimethylformamide (DMF; 20 mL) was vigorously stirred for 4 h. The resulting solution (pH = 3.2) was filtered and allowed to slowly evaporate. After 1 week, colorless block-shaped crystals were obtained. Yield: 69% based on Pb salt. Anal. Calcd for $C_{20}H_{19}N_3O_7PbS$: C, 36.81; H, 2.93; N, 6.44. Found: C, 36.94; H, 3.01; N, 6.41. IR (KBr pellet, cm^{-1}): 3405(m), 3065(w), 1632(m), 1590(s), 1574(s), 1490(m), 1478(m), 1439(s), 1388(m), 1316(w), 1212(s), 1178(s), 1127(m), 1084(m), 1035(s), 1010(m), 824(m), 773(s), 733(w), 676(s), 646(m), 602(s), 586(m), 406(w).

Synthesis of [Pb(Hssal)(2,2′-bipy)(H_2O)]$_n$ (2). A mixture of $Pb(CH_3COO)_2 \cdot 3H_2O$ (0.077 g, 0.20 mmol), 5-sulfosalicylic acid dihydrate (0.051 g, 0.20 mmol), 2,2′-bipy (0.031 g, 0.20 mmol), and water (10 mL) was placed in a 25-mL Teflon-lined reaction vessel (pH = 3.7) and heated under autogenous pressure at 413 K for 3 days. The vessel was then slowly cooled to room temperature. Several hours later needle crystals were grown from the resulting pink solution. Yield: 87% based on Pb salt. Anal. Calcd for $C_{17}H_{14}N_2O_7PbS$: C, 34.17; H, 2.36; N, 4.69. Found: C, 34.31; H, 2.56; N, 4.78. IR (KBr pellet, cm^{-1}): 3399(m), 3103(m), 1619(m), 1590(s), 1478(m), 1438(s), 1374(w), 1350(w), 1321(m), 1246(m), 1211(s), 1197(s), 1179(m), 1160(s), 1127(s), 1077(m), 1031(s), 1009(m), 895(w), 847(w), 818(w), 764(m), 734(m), 672(s), 643(w), 596(s), 569(w), 451(w), 407(m).

Synthesis of [Pb(Hssal)(phen)(DMF)]$_n$ (3). $Pb(CH_3COO)_2 \cdot 3H_2O$ (0.181 g, 0.48 mmol) and 1,10-phenanthroline monohydrate (0.101 g, 0.51 mmol) were dissolved in DMF (20 mL), and 5-sulfosalicylic acid dihydrate (0.126 g, 0.50 mmol) and NaOH (0.021 g, 0.53 mmol) were dissolved in water (10 mL). Then the solutions with pH = 5.9 were mixed and allowed to evaporate. After 5 days, colorless block crystals were obtained. Yield: 75% based on Pb salt. Anal. Calcd for $C_{22}H_{19}N_3O_7PbS$: C, 39.05; H, 2.83; N, 6.21. Found: C, 39.07; H, 2.77; N, 6.20. IR (KBr pellet, cm^{-1}): 3448(w), 3059(w), 2926(w), 1661(s), 1620(m), 1577(s), 1571(w), 1476(m), 1446(s), 1432(m), 1387(w), 1375(w), 1338(m), 1298(w), 1257(m), 1233(m), 1207(w), 1159(s), 1120(m), 1097(m), 1074(m), 1035(m), 1018(s), 895(w), 855(m), 820(w), 730(m), 668(m), 596(s), 567(w), 405(w).

Synthesis of [Pb_3(ssal)$_2$(phen)$_3$]$_n$ (4). A mixture of $Pb(CH_3COO)_2 \cdot 3H_2O$ (0.077 g, 0.20 mmol), 5-sulfosalicylic acid dihydrate (0.050 g, 0.20 mmol), 1,10-phenanthroline monohydrate (0.041 g, 0.021 mmol), NaOH (0.025 g, 0.63 mmol), and water (10 mL) was heated in a 25-mL Teflon-lined reaction vessel (pH = 6.1) at 433 K for 3 days. The vessel was then slowly cooled to room temperature. Yellow block crystals were isolated by filtration. Yield: 81% based on Pb salt. Anal. Calcd for $C_{50}H_{30}N_6O_{12}Pb_3S$: C, 37.71; H, 1.90; N, 5.28. Found: C, 37.72; H, 1.74; N, 5.33. IR (KBr pellet, cm^{-1}): 3456(m), 3053(m), 1588(s), 1561(s), 1538(s), 1512(s), 1458(s), 1424(s), 1375(m), 1313(s), 1247(s), 1149(s), 1117(s), 1097(m), 1078(m), 1015(s), 998(s), 906(w), 850(m), 840(m), 816(w), 803(w), 724(s), 661(m), 636(w), 596(s), 576(m), 415(w).

Single-Crystal Structure Determination. Crystals directly grown from the reaction medium with suitable sizes of **1**−**4** were selected for data collection by a Bruker Smart CCD area detector with graphite-monochromatized Mo Kα radiation ($\lambda = 0.710\,73$ Å). The data were integrated by use of the *SAINT* program,[13] and this program also did the intensities corrected for Lorentz and polarization effects. The absorption was done by the *SADABS* program.[14] The structures were solved by the heavy-atom method and successive Fourier syntheses. Once the heavy-atom peak had been located in the Patterson map, a Fourier synthesis was performed to locate the other non-H atoms. Full-matrix least-squares refinements on F^2 were carried out using the *SHELXL-97* package.[15] All non-H atoms were anisotropically refined. In compound **2**, the atom O5 is disordered and was refined using a separate partial model. H atoms on C atoms were placed in idealized positions and refined as riding atoms, with C−H = 0.93 Å and $U_{iso}(H) = 1.2U_{eq}(C)$. H atoms bound to O atoms were located in difference Fourier maps and refined with distance restraints of O−H = 0.85(1) Å and a fixed isotropic displacement parameter of $U_{iso}(H) = 0.08$ Å^2. The drawings of the molecules were realized with the help of ORTEP-3 for Windows. All of the programs used are included in the WinGX Suite with version 1.70.[16] Information concerning the crystallographic data collection and structure refinements is summarized in Table 1.

Results and Discussion

Reaction Chemistry. Initially, compound **1**, which associates with the coordination of the DMF molecule, was synthesized in DMF/H_2O by a typical solution-mixed method. Self-assembled frameworks largely depend on the synthesis conditions, such as starting materials, solvents, reaction temperature, pH, and molar ratio.[17−19] Therefore, we tried to replace DMF in **1** by other solvents to produce new frameworks, such as methanol, while in the mixed solvents of MeOH/H_2O used in the Pb^{2+}/2,2′-bipy/H_3ssal system, there are no suitable crystals precipitated, and only poor-quality crystals or cotton-like solids formed, which are different from compound **1** and subsequent compound **2** (confirmed by IR). Then hydrothermal synthesis was introduced into the Pb^{2+}/2,2′-bipy/H_3ssal system, resulting in the formation of compound **2**. Following the successful synthesis of compounds **1** and **2**, many tries for the Pb^{2+}/phen/H_3ssal system in DMF/H_2O or MeOH/H_2O at room temperature only formed the previously reported dimeric compound (confirmed by IR and single-crystal X-ray analysis) **5**,[3a] and further investigations on this system using dimethyl sulfoxide, methanol, ethanol, or their combination by a typical mixed solution method or (solvo)hydrothermal reaction yielded nothing but the dimeric compound **5** (confirmed by IR). Therefore, a new idea, largely changing the solution pH, was employed in the synthesis of new compounds based

---

(13) *SAINT*, version 6.02a; Bruker AXS Inc.: Madison, WI, 2002.

(14) Sheldrick, G. M. *SADABS, Program for Bruker Area Detector Absorption Correction*; University of Göttingen: Göttingen, Germany, 1997.

(15) Sheldrick, G. M. *SHELXL-97, Program for Crystal Structure Refinement*; University of Göttingen: Göttingen, Germany, 1997.

(16) Farrugia, L. *J. Appl. Crystallogr.* **1999**, *32*, 837.

(17) (a) Go, Y. B.; Wang, X. Q.; Anokhina, E. A.; Jacobson, A. J. *Inorg. Chem.* **2005**, *44*, 8265. (b) Go, Y. B.; Wang, X. Q.; Anokihina, E. V.; Jacobson, A. J. *Inorg. Chem.* **2004**, *43*, 5360.

(18) Diaz, P.; Benet-Buchholz, J.; Vilar, R.; White, A. J. P. *Inorg. Chem.* **2006**, *45*, 1617.

(19) Lu, Y. L.; Wu, J. Y.; Chan, M. C.; Huang, S. M.; Lin, C. S.; Chiu, T. W.; Liu, Y. H.; Wen, Y. S.; Ueng, C. H.; Chin, T. M.; Huang, C. H.; Lu, K. L. *Inorg. Chem.* **2006**, *45*, 2430.

Table 1. Crystallographic Data and Refinement Parameters for Compounds **1**−**4**

	compound			
	1	**2**	**3**	**4**
empirical formula	$C_{20}H_{19}N_3O_7PbS$	$C_{17}H_{14}N_2O_7PbS$	$C_{22}H_{19}N_3O_7PbS$	$C_{50}H_{30}N_6O_{12}Pb_3S_2$
M_r	652.63	597.55	676.65	1592.49
cryst size (mm^3)	0.15 × 0.26 × 0.28	0.11 × 0.14 × 0.37	0.17 × 0.18 × 0.49	0.23 × 0.26 × 0.39
cryst syst	monoclinic	monoclinic	monoclinic	monoclinic
space group	$P2(1)/n$	$P2(1)/c$	$P2(1)/n$	$P2(1)/c$
a (Å)	11.4282(7)	12.487(1)	11.4005(5)	11.7889(7)
b (Å)	16.1696(9)	7.7435(6)	15.2010(7)	21.5596(12)
c (Å)	11.5471(7)	18.6162(15)	12.6626(6)	18.6853(10)
α (deg)	90.00	90.00	90.00	90.00
β (deg)	91.530(1)	99.537(1)	94.627(1)	106.247(1)
γ (deg)	90.00	90.00	90.00	90.00
V (A^3)	2133.02(2)	1775.18(4)	2187.26(2)	4559.47(15)
Z	4	4	4	4
D_c ($g{\cdot}m^{-3}$)	2.03	2.24	2.05	2.32
μ (mm^{-1})	8.056	9.667	7.861	11.216
θ range	2.2−26.1	2.8−25.6	2.1−25.5	1.5−25.5
unique reflns	4227	3332	4057	8455
obsd reflns	3713	3005	3632	7085
no. of param	292	280	310	658
F(100)	1256	1136	1304	2983
T (K)	293 ± 2	293 ± 2	293 ± 2	293 ± 2
R1, wR2 [$I > 2\sigma(I)$]	0.024, 0.056	0.022, 0.053	0.022, 0.055	0.031, 0.073
R1, wR2 [all data]	0.029, 0.058	0.026, 0.054	0.026, 0.056	0.040, 0.077
GOF	1.037	1.057	1.080	1.063
largest peak and hole ($e{\cdot}Å^{-3}$)	0.753, −0.683	0.737, −0.627	0.970, −0.393	0.794, −1.288

Scheme 1

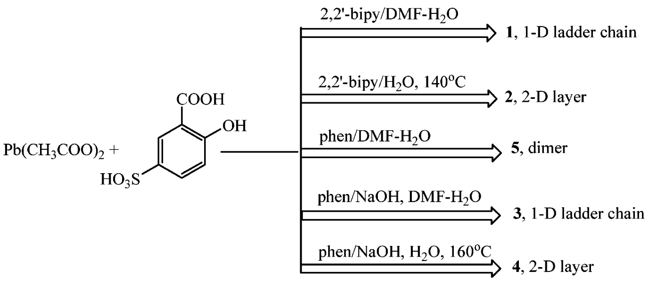

on the Pb^{2+}/phen/H_3ssal system. As expected, compounds **3** and **4** under the addition of NaOH were obtained by a typical solution-mixed method and hydrothermal reaction, respectively. These compounds are insoluble in water and common organic solvents, such as methanol, ethanol, acetone, and DMF. Therefore, crystals used for data collection were directly grown from the reaction medium. The pH values in the syntheses of compounds **1**−**4** need not be very precise, but the procedures reported in this presentation are suitable for the formation of good-quality crystals. The formation pathway of compounds **1**−**5** is shown in Scheme 1.

IR Spectra. In the spectra of compounds **1**−**5**, both COOH and SO_3H characteristic peaks near 1680 cm^{-1} are absent, indicating that these functional groups are deprotonated. In the region where ν(O−H) phenoxo deformation occurs, two absorption bands are observed at 1478 and 1439 cm^{-1} for **1**, at 1478 and 1438 cm^{-1} for **2**, at 1476 and 1446 cm^{-1} for **3**, and at 1487 and 1447 cm^{-1} for **5**, respectively. Compound **4** lacks such similar peaks. In a recent reference,[3c] a peak near 1627 cm^{-1}, which also occurs at 1632 cm^{-1} in **1**, at 1619 cm^{-1} in **2**, at 1620 cm^{-1} in **3**, and at 1629 cm^{-1} in **5**, was attributed to the ν(C−C) vibration, but this peak is absent in compound **4**; therefore, such a peak may be attributed to the vibration of O−H ($Hssal^{2-}$). In the IR spectra of **2** and **5**, the ν(O−H) stretching frequency of the broad band around 3400 cm^{-1} indicates the presence of a coordinated H_2O molecule. The IR spectra of **1**−**3** and **5** show typical asymmetric and symmetric carboxylate stretching bands at 1574 and 1388 cm^{-1} for **1**, at 1590 and 1321 cm^{-1} for **2**, at 1577 and 1387 cm^{-1} for **3**, and at 1574 and 1347 cm^{-1} for **5**, respectively. Unexpectedly, asymmetric and symmetric carboxylate stretching bands in **4** occur at 1561 and 1538 cm^{-1} and at 1424 and 1375 cm^{-1}, indicating that the carboxylates act as chelating−bridging coordination modes. The characteristic vibrations of SO_3^- in **1**−**5** are at 1212, 1178, and 1127 cm^{-1} in **1**, at 1211, 1179, and 1127 cm^{-1} in **2**, at 1233, 1159, and 1120 cm^{-1} in **3**, at 1247, 1149, and 1117 cm^{-1} in **4**, and at 1211, 1179, and 1127 cm^{-1} in **5** for $\nu_{as}(SO_3)$, respectively, whereas they are at 1035 cm^{-1} in **1**, at 1031 cm^{-1} in **2**, at 1035 cm^{-1} in **3**, at 1015 and 998 cm^{-1} in **4**, and at 1034 cm^{-1} in **5** for $\nu_{as}(SO_3)$, respectively.

Description of the Molecular Structures. Single-crystal X-ray analyses revealed that compounds **1** and **3** are isostructural. These two crystal structures demonstrate them to be 1-D ladderlike polymers. In **1** and **3**, each Pb^{II} atom is heptacoordinated by two N donors from one aromatic amine ligand (2,2′-bipy in **1** and phen in **3**), four O atoms from three $Hssal^{2-}$ ligands, and one DMF molecule (Figures 1 and 2). The selected bond distances and angles for **1** and **3** are listed in Table 2. The average distances of Pb−N in **1** and **3** are 2.494(3) and 2.507(3) Å, respectively, which are in good agreement with the reported values.[20−25] The carboxyl group of each $Hssal^{2-}$ ligand chelates to the Pb

---

(20) Shi, Y. J.; Li, L. H.; Li, Y. Z.; Chen, X. T.; Xue, Z. L.; You, X. Z. *Polyhedron* **2003**, *22*, 917.

(21) Soudi, A. A.; Marandi, F.; Morsali, A.; Zhu, L. G. *Inorg. Chem. Commun.* **2005**, *8*, 773.

(22) Tandon, S. S.; Mckee, V. *J. Chem. Soc., Dalton Trans.* **1989**, 19.

(23) Bazzicalupi, C.; Benicini, A.; Fusi, V.; Giorgi, C.; Paoletti, P.; Valtancoli, B. *J. Chem. Soc., Dalton Trans.* **1999**, 393.

(24) Tei, L.; Blake, A. J.; Bencini, A.; Valtancoli, B.; Wilson, C.; Schroder, M. *Inorg. Chim. Acta* **2002**, *337*, 59.

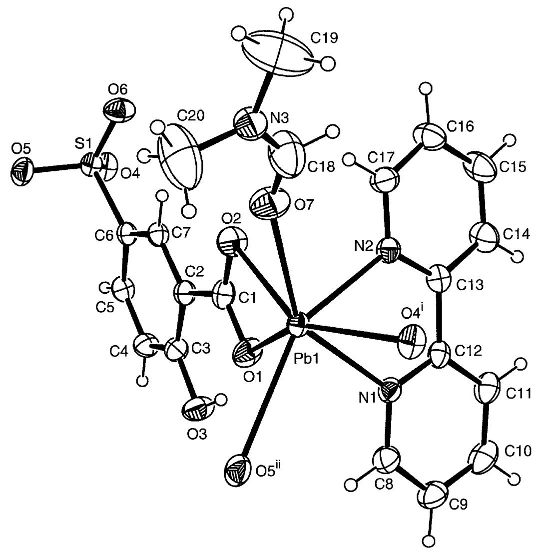

Figure 1. ORTEP plot (40% probability ellipsoids) of the asymmetric unit of compound **1** with the numbering scheme.

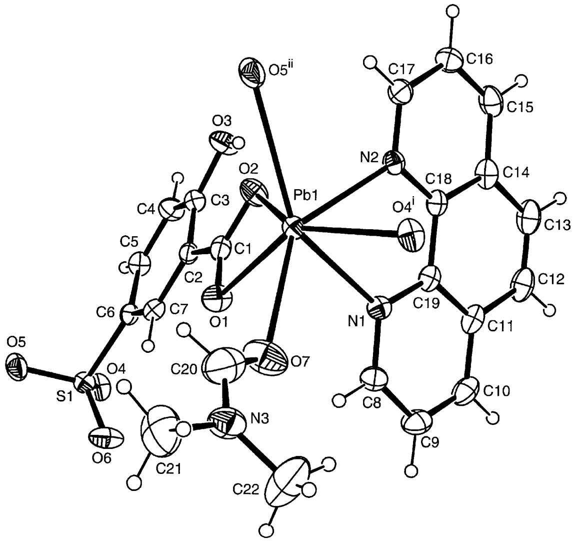

Figure 2. ORTEP representation of the asymmetric unit of compound **3**. The thermal ellipsoids are drawn at 40% probability.

Table 2. Selected Bond Lengths (Å) and Angles (deg) for Compounds **1**−**4**[a]

	Compound **1**		
Pb1−O1	2.493(3)	Pb1−O2	2.766(3)
Pb1−O4^{i}	2.616(3)	Pb1−O5^{ii}	2.929(3)
Pb1−O7	2.692(3)	Pb1−N1	2.523(3)
Pb1−N2	2.465(3)		
O1−Pb1−O2	49.32(8)	O1−Pb1−O4^{i}	146.56(9)
O1−Pb1−O5^{ii}	78.60(10)	O1−Pb1−O7	126.79(10)
O1−Pb1−N1	72.74(10)	N2−Pb1−O1	91.08(11)
O4^{i}-Pb1−O2	147.39(9)	O2−Pb1−O5^{ii}	117.98(9)
O7−Pb1−O2	79.29(10)	N1−Pb1−O2	105.28(11)
N2−Pb1−O2	72.57(10)	O4^{i}-Pb1−O5^{ii}	94.55(9)
O4^{i}-Pb1−O7	84.08(10)	N1−Pb1−O4^{i}	74.02(10)
N2−Pb1−O4^{i}	78.14(10)	O7−Pb1−O5^{ii}	124.76(10)
N1−Pb1−O5^{ii}	84.12(9)	N2−Pb1−O5^{ii}	149.18(9)
N1−Pb1−O7	145.39(11)	N2−Pb1−O7	84.66(11)
N2−Pb1−N1	65.06(10)		
	Compound **2**		
Pb1−O1	2.495(3)	Pb1−O2	2.731(3)
Pb1−O4^{i}	2.798(4)	Pb1−O6^{ii}	2.909(4)
Pb1−O7	2.588(4)	Pb1−N1	2.610(3)
Pb1−N2	2.616(3)		
O1−Pb1−O2	49.78(9)	O1−Pb1−O4^{i}	153.75(13)
O1−Pb1−O6^{ii}	105.33(10)	O1−Pb1−O7	79.27(11)
O1−Pb1−N1	81.66(11)	O1−Pb1−N2	90.38(11)
O2−Pb1−O4^{i}	153.18(13)	O2−Pb1−O6^{ii}	80.94(10)
O7−Pb1−O2	121.22(10)	N1−Pb1−O2	113.61(11)
N2−Pb1−O2	74.67(11)	O4^{i}-Pb1−O6^{ii}	94.69(11)
O7−Pb1−O4^{i}	84.78(13)	N1−Pb1−O4^{i}	74.98(12)
N2−Pb1−O4^{i}	89.07(12)	O7−Pb1−O6^{ii}	87.91(11)
N1−Pb1−O6^{ii}	164.29(11)	N2−Pb1−O6^{ii}	130.93(11)
O7−Pb1−N1	79.49(11)	O7−Pb1−N2	141.09(11)
N1−Pb1−N2	61.85(11)		
	Compound **3**		
Pb1−O1	2.655(3)	Pb1−O2	2.550(3)
Pb1−O4^{i}	2.645(3)	Pb1−O5^{ii}	2.901(3)
Pb1−O7	2.690(4)	Pb1−N1	2.478(3)
Pb1−N2	2.536(3)		
O2−Pb1−O1	50.10(8)	O4^{i}-Pb1−O1	145.01(9)
O1−Pb1−O5^{ii}	115.85(9)	O1−Pb1−O7	78.50(10)
N1−Pb1−O1	75.12(10)	N2−Pb1−O1	109.55(9)
O2−Pb1−O4^{i}	145.23(9)	O2−Pb1−O5^{ii}	78.56(9)
O2−Pb1−O7	128.59(10)	N1−Pb1−O2	86.21(10)
N2−Pb1−O2	70.41(9)	O4^{i}-Pb1−O5^{ii}	99.14(9)
O4^{i}-Pb1−O7	77.89(11)	N1−Pb1−O4^{i}	75.78(9)
N2−Pb1−O4^{i}	75.10(9)	O7−Pb1−O5^{ii}	133.63(11)
N1−Pb1−O5^{ii}	144.50(9)	N2−Pb1−O5^{ii}	78.73(9)
O7−Pb1−N1	80.43(12)	O7−Pb1−N2	140.92(12)
N1−Pb1−N2	65.94(10)		
	Compound **4**		
Pb1−O1	2.347(4)	Pb1−O3	2.414(4)
Pb1−O5^{i}	2.866(5)	Pb1−O9	2.806(4)
Pb1−N1	2.519(5)	Pb1−N2	2.603(5)
Pb2−O1	2.582(4)	Pb2−O2	2.775(4)
Pb2−O7	2.443(4)	Pb2−O9	2.429(4)
Pb2−O10^{iv}	2.997(5)	Pb2−O11^{ii}	2.903(4)
Pb2−N3	2.664(5)	Pb2−N4	2.609(5)
Pb3−O3^{ii}	2.868(4)	Pb3−O5^{iii}	2.574(4)
Pb3−O7	2.695(4)	Pb3−O8	2.395(4)
Pb3−O10^{iv}	2.751(4)	Pb3−N5	2.579(5)
Pb3−N6	2.578(5)		

[a] Symmetry codes for **1**: i, $x, y, -1 + z$; ii, $1 - x, -y, -1 - z$. Symmetry codes for **2**: i, $x, -y + {}^{1}/_{2}, -{}^{1}/_{2} + z$; ii, $-x, -{}^{1}/_{2} + y, {}^{1}/_{2} - z$. Symmetry codes for **3**: i, $1 + x, y, z$; ii, $1 - x, -y, -z$. Symmetry codes for **4**: i, $x, -y + {}^{1}/_{2}, -{}^{1}/_{2} + z$; ii, $-1 + x, y, z$; iii, $-1 + x, {}^{1}/_{2} - y, {}^{1}/_{2} + z$; iv, $x, {}^{1}/_{2} - y, {}^{1}/_{2} + z$.

atom with bond distances of 2.493(3) and 2.766(3) Å in **1** and 2.550(3) and 2.655(3) Å in **3**, respectively. Each DMF molecule is monodentally coordinated to the Pb^{II} atom with the Pb−O distances of 2.692(3) and 2.690(4) Å in **1** and **3**, respectively, and these values are much longer than that in [Pb(bipy)(DMF)($B_{10}H_9OH$)]·DMF[26] but similar to that in ($Pr_3N-C_2H_4-NPr_3$)[Pb(DMF)$_6$][Pb_5I_{14}]·DMF.[27] There are two different types of Pb−O(sulfonyl) bond distances in **1** and **3**. The shorter bond distances are 2.616(3) Å in **1** and 2.645(3) Å in **3**, whereas the longer bond distances are 2.929(3) Å in **1** and 2.901(3) Å in **3**, respectively. As discussed in refs 21 and 28,[21,28] a search of the bond distances for Pb−O up to 3.07 or 3.10 Å is reasonable and usually can find a nearly ideal value assumed for oxidation state II on

---

(25) Datta, B.; Adhikary, B.; Bag, P.; Florke, U.; Nag, K. *J. Chem. Soc., Dalton Trans.* **2002**, 2760.
(26) Zhizhin, K. Y.; Vovk, O. O.; Malinina, E. A.; Mustyatsa, V. N.; Goeva, L. V.; Polyakova, N.; Kuznetsov, N. T. *Russ. J. Coord. Chem.* **2001**, *27*, 613.
(27) Krautscheid, H.; Vielsack, F.; Klaassen, N. *Z. Anorg. Allg. Chem.* **1998**, *624*, 807.
(28) Foreman, M. R. J.; Gelbrich, T.; Hursthouse, M. B.; Plater, M. J. *Inorg. Chem. Commun.* **2000**, *3*, 234.

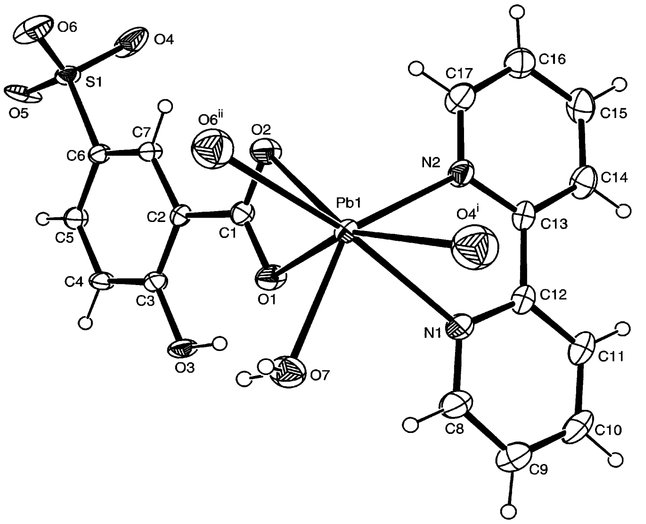

Figure 3. ORTEP diagram of the asymmetric unit of compound **2**. The thermal ellipsoids are drawn at 40% probability.

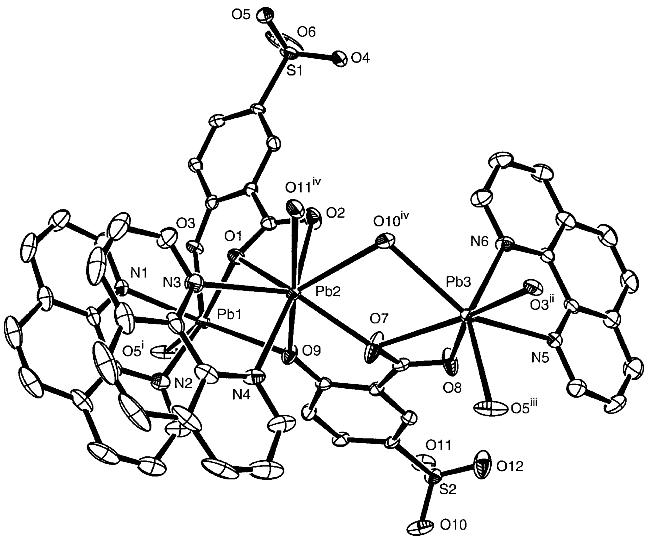

Figure 4. ORTEP view of the asymmetric unit of compound **4**. The thermal ellipsoids are drawn at 30% probability. H atoms are omitted for clarity.

Chart 3

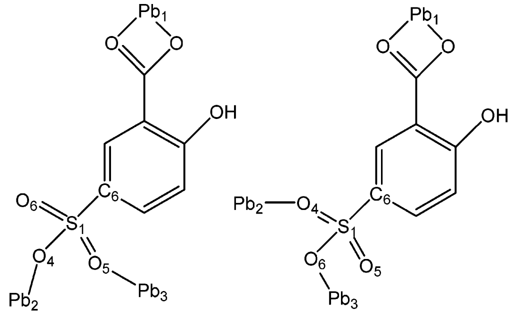

1 and **3** **2**

the Pb^{II} atom. Therefore, longer bond distances in **1** and **3** can be acceptable and are considered as weak bonding. Such comparable longer Pb−O bond distances can be easily found in recent references, for example, 3.058 Å in [Pb_2(2,2′-bipy)$_2$(μ-4,4′-bipy)(NO_3)$_4$][18] and 3.072 Å in [Pb_3(BTC)$_2$].[25]

Each Hssal^{2-} ligand performs a μ_3-coordination mode in **1** and **3**; therefore, ladderlike chains were formed in which the separations of Pb···Pb by sulfonates are 5.0943(4) Å for **1** and 4.9807(3) Å for **3**, respectively. Moreover, the separations of Pb···Pb by Hssal^{2-} ligands in the ladderlike chains are 8.5681(5) and 11.5471(7) Å for **1** and 8.2893(4) and 11.4005(5) Å for **3**, respectively, which are longer than those in the dimer **5**.[3a]

Determination of the structure of **2** by X-ray crystallography shows compound **2** in the solid state to be a 2-D double-sheet network. As shown in Figure 3, the Pb^{II} ion is chelated by two N atoms of one 2,2′-bipy ligand, four O atoms from three Hssal^{2-} ligands, and one O atom from one H_2O molecule. The Pb−N bond distances in **2** are much longer than those of **1**, while the Pb−O7(water) bond distance is similar to that in **5**.[3a] The carboxyl group chelates to the Pb atom with similar values found in compounds **1** and **3**. The coordination number in **2** is 7 with a PbN_2O_5 chromophore. The distances of Pb···Pb separated by the Hssal^{2-} ligand are 9.4066(7) and 10.0091(6) Å, while the Pb···Pb separation by sulfonate is 5.3279(4) Å. The two rings of the 2,2′-bipy ligand in **2** are nearly coplanar with a dihedral angle of 2.1(2)°, which is similar to that in compound **1** [3.0(1)°]. Each Hssal^{2-} ligand acts as a chelating−bridging mode in the μ_3 form, but such a mode is very different from those in **1** and **3**. In contrast to the syn-bridging mode of each sulfonate group in **1** and **3**, each sulfonate in **2** is antibridging. Therefore, in **1** and **3** the extended frameworks are 1-D ladderlike chains, whereas in **2**, the extended network is 2-D double-layer architecture. In these compounds **1**−**3**, the hydroxyl groups of Hssal all are nonbonding and all sulfonates are coordinated to Pb^{II} atoms through two O atoms. The coordination modes of Hssal^{2-} in **1**−**3** are shown in Chart 3, in which the torsion angles of Pb2−O4−S1−C6 and Pb3−O5−S1−C6 are −126.7(2)° and +18.3(2)° for **1** and −117.9(2)° and +14.5(2)° for **3**, respectively, while the torsion angles of Pb3−O6−S1−C6 and Pb2−O4−S1−C6 in **2** are −103.7(2)° and −140.2(2)°, respectively.

In **1**−**3**, each Hssal^{2-} is doubly deprotonated, while in **4**, each ssal^{3-} is fully deprotonated. Single-crystal X-ray analysis reveals that compound **4** possesses a 2-D polymeric structure where there are three types of Pb^{II} ions in an asymmetric unit with coordination numbers 6 for Pb1, 8 for Pb2, and 7 for Pb3. As shown in Figure 4, Pb1 is coordinated by two N atoms of one phen ligand and four O atoms (O1, O3, O9, and O5^{i}) from three ssal^{3-} ligands. Pb2 is coordinated by two N atoms of one phen ligand and six O atoms (O1, O2, O7, O9, O10^{iv}, and O11^{iv}) from four ssal^{3-} ligands. Pb3 is coordinated by two N atoms from one phen ligand and five O atoms (O3^{ii}, O5^{iii}, O7, O8, and O10^{iv}) from four ssal^{3-} ligands. Pb−N bond distances except Pb1−N1 and Pb2−N2 in **4** are similar and can be found in [Pb(phen)$_2$(CH_3COO)](ClO_3)[29] but are longer than those of **3**. All bond distances of Pb−O(COO^-) in **4** are in the typical range of 2.347(4)−2.775(4) Å.

The fully deprotonated 5-sulfosalicylates in **4** perform two novel coordination modes (Chart 4), which are not reported

---

(29) Morsali, A.; Mahjoub, A. R.; Darzi, S. J.; Soltanian, M. J. *Z. Anorg. Allg. Chem.* **2003**, *629*, 2596.

Chart 4

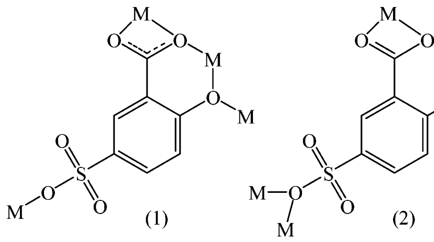

Chart 5. Projection of the Coordination Spheres of Pb^{II} Ions in Compounds **1**−**4**

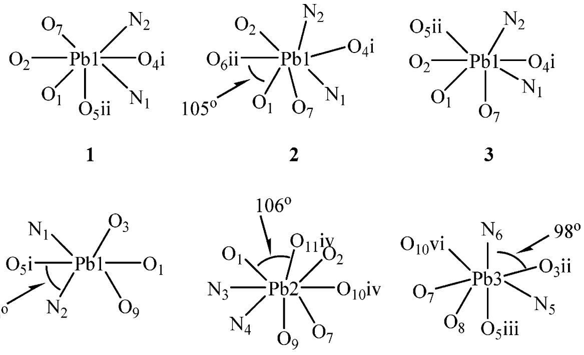

1 **2** **3**

4 **4** **4**

Table 3. H-Bonding Geometry Parameters (Å and deg) for Compounds **1**−**3**[a]

D−H···A	D−H	H···A	D···A	D−H···A
		Compound **1**		
O3−H3A···O1	0.847(10)	1.71(2)	2.508(4)	157(5)
		Compound **2**		
O3−H3A···O1	0.848(10)	1.81(4)	2.553(4)	145(6)
O7−H7A···$O5^{i}$	0.85(1)	2.02(4)	2.697(17)	136(5)
O7−H7B···$O6^{ii}$	0.848(10)	2.35(4)	2.911(6)	124(4)
O7−H7B···$O3^{iii}$	0.848(10)	2.42(2)	3.216(5)	156(4)
		Compound **3**		
O3−H3···O2	0.82	1.80	2.526(4)	146.9

[a] Symmetry codes in **2**: i, $x, -y + {}^3/_2, z - {}^1/_2$; ii, $x, -y + {}^1/_2, z - {}^1/_2$; iii, $-x, -y + 1, -z$.

Table 4. Aromatic−Aromatic Interactions in Compound **4**[a]

no.	two rings	centroid-to-centroid distance (Å)	symmetry code
1	1, 7	3.712(4)	$2 - x, {}^1/_2 + y, {}^1/_2 - z$
2	2, 4	3.685(5)	x, y, z
3	2, 8	3.613(5)	x, y, z
4	3, 9	3.550(5)	x, y, z
5	4, 7	3.628(4)	$1 - x, {}^1/_2 + y, {}^1/_2 - z$
6	5, 8	3.612(5)	$1 - x, -{}^1/_2 + y, {}^1/_2 - z$
7	6, 9	3.664(4)	$2 - x, -{}^1/_2 + y, {}^1/_2 - z$

[a] Ring 1: N1, C8−C11, C19. Ring 2: N2, C14−C18. Ring 3: N3, C27−C30, C38. Ring 4: N4, C33−C37. Ring 5: N5, C39−C42, C50. Ring 6: N6, C45−C49. Ring 7: C42−C45, C49−C50. Ring 8: C30−C33, C37−C38. Ring 9: C11−C14, C18−C19.

in the references. Each carboxyl group acts as chelating and bridging modes (totally tridentate) where the two O atoms coordinate to a Pb^{II} ion and one of them is also involved in a bridge to an adjacent Pb^{II} ion. The phenolate and sulfonate groups act as one-atom bridging or monodentate modes, respectively. Therefore, the extended framework of **4** is a 2-D architecture.

It is interesting that there is a weak Pb···Pb interaction [4.0711(4) Å] between Pb1 and Pb3 in **4**, which can be compared to the reported values.[30,31] In the trinuclear motif, several separations of Pb···Pb can be found; i.e., Pb1 and Pb2 are bridged by a carboxyl O atom with a Pb···Pb distance of 4.5183(4) Å. The distance between Pb2 and Pb3 separated by the $ssal^{3-}$ ligand is 8.0902(6) Å. Pb2 and Pb3 are also bridged by two O atoms of the phenolate and sulfonate groups, forming a Pb_2O_2 unit with a Pb···Pb distance of 4.277(4) Å.

The stereochemical activity of the lone pair of electrons is an interesting issue, which is always discussed. Shimoni-Livny and co-workers classify Pb^{II} complex geometries as holo- and hemidirected.[5] Holodirected refers to Pb^{II} complexes in which the bonds to ligand atoms are placed throughout the surface of the encompassing globe, while hemidirected refers to those cases in which the bonds to ligand atoms are directed throughout only part of an encompassing globe. In compounds **1** and **3**, the lone pairs of electrons are clearly inactive; thus, the coordination spheres of Pb^{II} ions are holodirected. In contrast to **1** and **3**, the coordination spheres of Pb^{II} ions in **2** and **4** feature small holes or gaps; therefore, these coordination spheres can be considered as somewhat hemidirected (Chart 5).

In compounds **1**−**3**, the carboxyl groups with their attached benzene rings have nearly coplanar arrangements, and their dihedral angles are 1.69(4)°, 1.7(4)°, and 4.29(14)°, respectively; interestingly, carboxyl groups in these compounds are localized. In contrast, the dihedral angles between the benzene ring and the carboxyl group in compound **4** are significantly large, with values of 16.5(8)° and 26.8(4)°, indicating novel structural features in the solid-state assembly.

In general, Pb^{II} complexes are solvent-poor species and compounds **1**−**4** also exhibit such a property. Therefore, these four compounds only feature a few H-bonding interactions. There is no H bonding in compound **4**, and H bonds in compounds **1**−**3** only occur within the chains or layers (Table 3).

The weak $\pi-\pi$ interactions occur between rings of symmetry-related 2,2′-bipy ligands from adjacent chains in **1**, with a centroid distance of 3.958(3) Å (symmetry code: $2 - x, -y, -z$). In compound **2**, $\pi-\pi$ stack interactions exist between rings of symmetry-related 2,2′-bipy ligands from adjacent layers, with the centroid distances of 3.605(3) and 3.758(3) Å (symmetry codes: $1 - x, -y, -z$; $1 - x, 1 - y, -z$). Compounds **1** and **3** share the same topological ladderlike chain, but in compound **3**, the strong $\pi-\pi$ stacks can be observed between rings of symmetry-related phen ligands with a centroid distance of 3.439(2) Å (symmetry code: $2 - x, -y, 1 - z$) because the phen ligand is sterically rigid with three rings compared to the 2,2′-bipy ligand. In contrast to compounds **1**−**3**, in compound **4** there are extensively $\pi-\pi$ stacking interactions between benzoates or phen ligands that are within or between layers (Table 4).

Removal of Solvated Molecules. Differential thermal analyses (DTA)−TGA for compounds **1**−**3** were performed under a flow of N_2 gas. For **1**, the first-step weight loss of

---

(30) Xiao, H. P.; Morsali, A. *Helv. Chim. Acta* **2005**, *88*, 2543.
(31) Morsali, A.; Mahjoub, A. R. *Helv. Chim. Acta* **2004**, *87*, 2717.

10.96% (calcd 11.20%) from 190 to 220 °C accompanied by an endothermic peak corresponds to the removal of one DMF molecule per formula unit. Compound **1** decomposes at 311 °C. Compound **2** releases the coordinated H_2O molecule from 150 to 200 °C with a weight loss of 3.25% (calcd 3.01%). Compound **2** decomposes at 293 °C. TGA for compound **3** show that one DMF molecule was lost in the temperature range 150−220 °C (calcd 10.80%; obsd 9.41%) and this compound decomposes at 339 °C.

Photoluminescence. The solid-state photoluminescent spectra of compounds **1**−**4** at room temperature upon excitation at 220 nm have been measured. The maximum emission occurs at 408 nm for **1** and 407 nm for **3**, corresponding to the $S_0 \rightarrow S_1$ absorption, but such an emission is not found in **2** and **4**, which may be attributed to the enhancing influence of the coordinated DMF molecule on emission. Moreover, there is a strong emission at 470 nm in all four compounds (for compounds **2** and **4**, this emission is a maximum one), which is red-shifted about 20 nm compared to that of free H_3ssal ligand (450 nm). Obviously, this strong emission comes from the 5-sulfosalicylate ligand, and the large red-shifted effect may be attributed to the coordination or an excited state of a metal-perturbing intraligand.

Conclusion

We have synthesized four lead(II) 5-sulfosalicylate compounds. Assemblies and diverse structural topologies of these four compounds largely depend on the solvents, solution pH, and synthetic methods. Structural analyses and characterizations of these four compounds give us some valuable information. First, assemblies of four compounds generate three types of diverse frameworks: a 1-D ladderlike chain, a 2-D double-layer architecture, and a 2-D layer network. Second, Hssal^{2-} and ssal^{3-} ligands perform novel coordination modes, which are not reported before. In **1**−**3**, Hssal^{2-} ligands act as chelating−bridging modes, while in contrast to the syn bridging mode of sulfonates in **1** and **3**, sulfonates in **2** serve as antibridging. Third, compounds in **1**−**4** are solvent-poor, containing, therefore, no H bonding in **4**, and only intrachain or intralayer H bonds can be observed in compounds **1**−**3**. Fourth, aromatic−aromatic stacking interactions in **1**−**3** can only be observed between rings of heterocyclic amine ligands. However, there are extensively $\pi-\pi$ interactions in compound **4**. Finally, weak Pb···Pb interactions can be observed in compound **4**, which is sparse in Pb^{II} complexes.

Acknowledgment. The authors thank the National Natural Science Foundation of China (Grant 50073019) and the Analytical and Measurement Fund of Zhejiang Province.

Supporting Information Available: X-ray crystallographic data in CIF format. This material is available free of charge via the Internet at http://pubs.acs.org.

IC060871V